

Alma Mater Studiorum Università di Bologna
Archivio istituzionale della ricerca

Preparation of gum acacia-poly(acrylamide-IPN-acrylic acid) based nanocomposite hydrogels via polymerization methods for antimicrobial applications

This is the final peer-reviewed author's accepted manuscript (postprint) of the following publication:

Published Version:

Sharma S., Virk K., Sharma K., Bose S.K., Kumar V., Sharma V., et al. (2020). Preparation of gum acacia-poly(acrylamide-IPN-acrylic acid) based nanocomposite hydrogels via polymerization methods for antimicrobial applications. JOURNAL OF MOLECULAR STRUCTURE, 1215, 1-12 [10.1016/j.molstruc.2020.128298].

Availability:

This version is available at: <https://hdl.handle.net/11585/760030> since: 2020-05-25

Published:

DOI: <http://doi.org/10.1016/j.molstruc.2020.128298>

Terms of use:

Some rights reserved. The terms and conditions for the reuse of this version of the manuscript are specified in the publishing policy. For all terms of use and more information see the publisher's website.

This item was downloaded from IRIS Università di Bologna (<https://cris.unibo.it/>).
When citing, please refer to the published version.

(Article begins on next page)

This is the final peer-reviewed accepted manuscript of:

SHARMA, S.; VIRK, K.; SHARMA, K.; BOSE, S. K.; KUMAR, V.; SHARMA, V.; FOCARETE, M. L.; KALIA, S. PREPARATION OF GUM ACACIA-POLY(ACRYLAMIDE-IPN-ACRYLIC ACID) BASED NANOCOMPOSITE HYDROGELS VIA POLYMERIZATION METHODS FOR ANTIMICROBIAL APPLICATIONS. JOURNAL OF MOLECULAR STRUCTURE 2020, 1215, 128298.

The final published version is available online at:
<https://doi.org/10.1016/j.molstruc.2020.128298>.

Terms of use:

Some rights reserved. The terms and conditions for the reuse of this version of the manuscript are specified in the publishing policy. For all terms of use and more information see the publisher's website.

This item was downloaded from IRIS Università di Bologna (<https://cris.unibo.it/>)

When citing, please refer to the published version.

Preparation of gum acacia-poly(acrylamide-ipn-acrylic acid) based nanocomposite hydrogels via polymerization methods for antimicrobial applications

Shikha Sharma^a, Karan Virk^b, Kashma Sharma^{a*}, Sunil Kumar Bose^c, Vijay Kumar^{d*}, Vishal Sharma^a, Maria Letizia Focarete^e, Susheel Kalia^{f*}

^aInstitute of Forensic Science & Criminology, Panjab University, Chandigarh, 160014, India

^bDepartment of Applied Physics, Chandigarh University, Gharuan, 140413, Punjab, India

^cDepartment of Microbiology, Panjab University, Chandigarh, 160014, India

^dDepartment of Physics, National Institute of Technology (NIT), Hazratbal-19006, Srinagar, J&K (India)

^eDepartment of Chemistry “G. Ciamician”, University of Bologna, via Selmi 2, 40126 Bologna, Italy

^fDepartment of Chemistry, Army Cadet College Wing of Indian Military Academy, Dehradun 248007 (Uttarakhand), India

*Corresponding authors: shama2788@gmail.com (K. Sharma); vj.physics@gmail.com (Vijay Kumar); sharmavishal05@gmail.com (V. Sharma); susheel.kalia@gmail.com (S. Kalia)

Abstract

An interpenetrating superabsorbent nanocomposite hydrogel based on gum acacia-acrylamide-acrylic acid (Ga-cl-poly(AAm-IPN-AA)) was synthesized by a two-step aqueous polymerization and one step impregnation methods. The first step comprises the preparation of a semi-interpenetrating Ga-cl-poly(AAm) network based on AAm and Ga via free radical polymerization. The reaction was initiated by ammonium persulphate under microwave irradiation and N, N'-methylene-bis-acrylamide was used as a crosslinker during the polymerization. The maximum percentage of swelling (1256%) was exhibited by the semi-

IPN. In the second step, the synthesis of IPN was carried out by the crosslinking of polyacrylic acid onto semi-interpenetrating hydrogel. The synthesized crosslinked hydrogels were studied by FTIR, SEM and XRD techniques. Silver nanoparticles (AgNPs) (20-80 nm) were synthesized from flower extract of *Koelreuteria apiculata* and synthesized hydrogels were employed as a template for the impregnation of AgNPs. The resultant nanocomposite superabsorbent was also studied by XRD, FTIR, and SEM techniques. The prepared samples were subjected to antibacterial and antifungal studies with different bacterial (*Staphylococcus aureus*, *Escherichia coli*, *Pseudomonas aeruginosa*) and fungal strains (*Aspergillus* and *Penicillium*). Synthesized nanocomposite hydrogels have shown improved antibacterial and antifungal activities.

Keywords: Silver nanoparticles, nanocomposite hydrogels, microwave irradiation, antimicrobial properties.

1. Introduction

Hydrogels are hydrophilic three-dimensional systems that possess water holding capacity owing to the presence of various functional groups like –OH, –CONH₂ and –SO₃H [1-3]. The hydration of hydrogel depends upon nature and environmental factors like pH, pressure, temperature and many other stimuli [4]. Hydrogels have numerous applications in various areas like the food industry, pharmaceuticals, agriculture and horticulture, biosensors, wastewater treatment, drilling fluid additives and biomedical implants [5-6].

A substantial amount of work is reported in the literature concerning the antibacterial applications of polysaccharide and their hydrogels. Vimala et. al [7] synthesized alginate-gum acacia-silver nanocomposite films for their utilization in food packaging and its antimicrobial activity was determined against numerous foodborne bacteria. Padmanabhan et. al [8] synthesized nanocomposites of hydroxyapatite and gum acacia for applications in drug

delivery and tissue engineering applications. They have attained a sustained drug release profile of naringenin. Additionally, antimicrobial activity was assessed against *Staphylococcus aureus* (*S. aureus*) and *Escherichia coli* (*E. coli*) turmeric nanofibres based nanocomposite hydrogels were synthesized to enhance the physicochemical properties of gum arabic, polyethylene glycol and maltodextrin. Antibacterial activity of nanocomposite was investigated against *E. coli*, *Salmonella typhimurium*, *Bacillus cereus* and *S. aureus* [9]. AgNPs were synthesized by in situ methods in the matrix of polyvinyl alcohol/gum acacia and antibacterial activity was investigated against *E. coli*. Synthesized nanocomposites showed promising antibacterial activity in the inhibition of bacterial growth [10]. Bajpai and Kumari [11] synthesized AgNPs-based gum acacia/poly(acrylate) nanocomposites for antibacterial applications. They also synthesized zinc oxide nanoparticles (ZnO NPs) loaded gum acacia/poly(SA) hydrogels by a hydrothermal method [12]. The antibacterial activity of ZnO NPs loaded polymer composites was studied by the ‘zone of inhibition’ method. They have also prepared poly(vinyl alcohol)/ZnO nanocomposites for wound dressing applications [13]. Cu nanoparticles based chitosan nanocomposite hydrogels were prepared for antimicrobial applications. The antimicrobial activity of the nanocomposite hydrogels was studied by the ‘zone of inhibition’ method against gram-negative and gram-positive bacteria. It has been observed that synthesized nanocomposite hydrogels showed better antimicrobial applications [14]. Antimicrobial collagen/chitosan/lysine hyaluronic acid-based hydrogels were fabricated for possible bone tissue engineering applications [15]. Synthesized hydrogels were found to be biocompatible, antibacterial and show favorable characteristics as prospective multifunctional scaffolds.

Gum acacia (Ga) is a complex, edible, soluble, branched polysaccharide of acidic nature that contains glucuronic acid, arabinose, galactose, rhamnose, remains consist of 1,3 beta –D-galactopyranosyl units. Gum acacia possesses antioxidant activity due to the presence of

hydrocolloids [16-18]. Ga is used in applications like liquor, confectionery or water-based emulsions, pharmaceutical, cosmetic products, inks, etc. [19]. Nanocomposite hydrogels can be prepared by joining the superior properties of nanoparticles and polymer matrix such as polysaccharides.

Plant polysaccharides are biodegradable, non-toxic, low cost, and renewable and can potentially be used as key ingredients for the production of nanocomposite hydrogels for mankind. Polysaccharide-based nanocomposite hydrogels have found extensive applications in various fields, including agriculture, wastewater treatment, electronics, and biomedical applications. Therefore, gum acacia was utilized in the present study for the development of antimicrobial nanocomposite hydrogels. Various reaction parameters like initiator concentration, amount of crosslinker, monomer concentration and amount of solvent were optimized to get the final sample with a maximum percentage of swelling and grafting. Further, antibacterial and antifungal activity of nanocomposite hydrogels were studied against gram-positive strain (*S. aureus*) and gram-negative strains of bacteria (*Pseudomonas aurengensis*, *E. coli*) and as well as against fungus (*Penicillium* and *Aspergillus*). The incorporation of silver nanoparticles to prepared hydrogel networks has shown a remarkable enhancement of antimicrobial activity.

2. Experimental

2.1 Materials

Gum acacia (Ga) was purchased from Sisco Research Laboratories Pvt. Ltd. Ammonium persulfate (APS) as initiator was procured from Sigma Aldrich. Acrylamide and acrylic acid was purchased from Loba Chemie Pvt Ltd. N,N'-methylenebisacrylamide (MBA) was purchased from Central Drug House Ltd. India. Silver nitrate salt was purchased from Merck Life Science Pvt Ltd.

2.2 *Synthesis of Ga-cl-poly(AAm)*

Gum acacia (0.5 g) was added to 14 ml distilled water and continuously stirred with a pre-weighed amount of initiator and monomer followed by the addition of crosslinker. The polymerization reaction was initiated under the influence of microwave radiation for a fixed duration of time. Various reaction parameters such as APS, AAm and MBA concentration were optimized to achieve the best percentage swelling. The homopolymer and impurities were removed by washing through double distilled water. The synthesized hydrogel was kept in a hot air oven overnight at 60 °C to get the final product.

2.3 *Synthesis of Ga-cl-poly(AAm-IPN-AA)*

The synthesis of Ga-cl-poly(AAm-IPN-AA) was initiated by taking the optimized amount of Ga-cl-poly(AAm) into the beaker. The pre-optimized amount of initiator and crosslinker was added with regular stirring. After the addition of acrylic acid, the resultant solution was kept for 23 hours at ambient temperature, which eventually results in the formation of the swollen sample. After 23 hours, the polymerization reaction was initiated by microwave irradiation. The concentration of acrylic acid was optimized. An unbounded homopolymer was washed off with distilled water. The resulting hydrogel was dried in a hot air oven overnight at 60 °C. Synthesis of Ga-cl-poly(AAm-IPN-AA) is depicted in Scheme 1.

2.4 *Preparation of silver nanoparticles*

Flowers of tree *Koelreuteria apiculata* were washed with distilled water for multiple times to carry off all the dirt particles followed by drying at room temperature. 5g of flowers were weighed and boiled in 200 ml distilled water for 6 minutes under microwave radiation. Flower extract was centrifuged at 6000 rpm for 10 minutes, followed by subsequent filtration with Whatman filter paper. The silver nitrate solution with varying concentrations of 1-5 mM was

prepared along with different concentrations (1-5 ml) of flower extracts [20]. The optimized concentration was found to be 2 mM of silver nitrate with 1ml of flower extract.

2.5 Preparation of nanocomposite hydrogels

Nanocomposite hydrogels were synthesized by the ex-situ method. Initially, 1g of crosslinked hydrogel was dipped in 10 ml of already prepared silver nanoparticles and no antibacterial activity was observed at this concentration. Therefore, the impregnation of silver nanoparticles into the hydrogels was done by dipping the 2g of already prepared Ga-cl-poly(AAm) and Ga-cl-poly(AAm-IPN-AA) in 60 ml of nanoparticles separately for 24 hours and afterward kept in a hot air oven for 24 hours to get the desired nanocomposite hydrogels.

2.6 Swelling properties

The swelling studies of the synthesized hydrogels were carried out by the well-reported procedure [21].

2.7 Characterization techniques

Synthesized hydrogels were characterized by Fourier Transformed Infrared (FTIR) spectrophotometer (Perkin Elmer) having diamond crystal and ZnSe for focusing element. Scanning electron micrographs of samples were taken on the JEOL JSM-6490LV microscope after the thin layer coating of samples with gold using D11-29030SCTR Smart Coater. The impregnation of silver nanoparticles in the hydrogels was determined using EDX spectra. XRD spectra were recorded using a Spinner PW3064, X'pert PRO diffractometer with Cu-K α of 1.54060 Å at the 2 θ scale ranging from 10°-80°. Silver nanoparticles were characterized using a UV2550 SHIMADZU CORP spectrophotometer.

2.8 *Antibacterial and antifungal studies*

The bacterial strains were taken from the Institute of Microbial Technology (IMTECH), Chandigarh to check the antimicrobial activities. Bacterial and fungal strains were incubated for 24 hours at 37°C on nutrient agar and potato dextrose agar (PDA) mediums, respectively. Stocks were maintained at 4°C.

2.8.1 *Agar well diffusion method*

The antibacterial activities of the backbone and synthesized hydrogels samples were studied by agar well diffusion assay as per the standard guidelines. The overnight bacterial culture was diluted (1:100) to obtain 10^5 CFU/ml for each bacteria to be tested (*S. aureus*, *E. coli* and *Pseudomonas aeruginosa*) and was spread using sterile swab consisting bacterial suspension on Muller Hinton Agar plates. Afterward, wells having dimensions of 6 mm diameter were punched into the agar plates comprising a bacterial suspension and filled with 50 mg/ml of gum acacia and hydrogels and retained at ambient temperature for 2 hours for diffusion. Subsequently, the plates were then incubated at 37°C for 24 hours. Wells containing the same amount of sample 'A' served as control. The diameters of zone of inhibition around the wells were measured in mm after an incubation of 24 hours, against all the above-mentioned organisms for three replicates.

2.8.2 *Antifungal activity*

The standard agar well diffusion technique was employed to check antifungal activity. The fungus was inoculated over the Potato Dextrose Agar medium with 1 ml of spore suspension. A sterile metal cylinder with a 6 mm diameter was used to punch wells in agar plates. The test samples were placed into them. The agar plates were left for 2 hours specifically at room temperature and then incubated under aerobic conditions at 28 °C for the diffusion of samples.

The zones of inhibition of fungal growth around the wells were measured in millimetres after the incubation period of 2-3 days.

3. Results and discussions

3.1 Synthesis of gum acacia-based nanocomposite hydrogels

Ga-acrylamide (AAM)-acrylic acid (AA) was prepared by a two-step aqueous polymerization under the influence of microwave irradiation. The proliferation of the reaction was initiated by the creation of reactive sites on gum acacia and monomer. Microwave irradiation causes the disintegration of ammonium persulfate and generates sulfate ion radicals. Water molecules present in the reaction system absorb microwave energy and rapidly produced $\cdot\text{OH}$ ion radicals. The free radicals were created on polar $-\text{OH}$ groups of gum acacia. Free radicals present in the adjacent vicinity of monomer molecules lead to chain initiation and propagation steps [22-23]. During the propagation, the polymer chain reacts to the end groups of crosslinker resulting in a crosslinked structure. Both semi-IPN and IPN with the maximum percentage of swelling were prepared at optimized reaction parameters.

The water uptake ability showed an increasing trend at the beginning with increasing the concentration of APS from 0.008 mol/L to 0.021mol/L due to an increased number of free radicals on the Gum acacia (Fig. 1a) [24]. The P_s was also examined with respect to the amount of concentration and maximum P_s was achieved with 14 ml of solvent. Thereafter, the water holding capacity of the grafted copolymer was found to decrease (Fig. 1b). The decreased P_s was due to the hindrance over the reaction chain due to the excess generation of hydroxyl free radicals in a large amount of solvent [25]. From Fig. 1c, it can be depicted that at 2.813 mol/L concentration of acrylamide showed the maximum P_s . The further increase brings out a decreasing trend in the P_s due to over protonation or self-crosslinking of monomer molecules [26-27]. The optimum amount of MBA also influences the swelling behavior of

synthesized hydrogels. The P_s was examined with changing concentrations of MBA from 0.006 mol/L to 0.032 mol/L. Fig. 1d reveals that the greatest extent of P_s was observed with 0.012 mol/L. A further rise in crosslinker concentration showed a reduced P_s due to a decrease in the dimension of pores on hydrogels. Also, a decrease in the flexibility of copolymer chains leads to stiffer network and do not permit a significant relaxation. This accounts for the decrease in water-absorbing capacity of synthesized hydrogels at higher concentrations [28-29].

The concentration of acrylic acid was optimized to get the Ga-cl-poly(AAm-IPN-AA) with maximum P_s at other preoptimized reaction parameters. The varying concentrations of acrylic acid from 0.00007 mol/L - 0.00029 mol/L were analyzed for this purpose (Fig. 1e). The P_s was decreasing with the increased concentration of AA due to the integration of elevated self-crosslinking [30]. A more packed and inelastic structure was resulted due to an overabundance of monomer in the reaction system, which eventually reduces the pore size and water holding capacity of the hydrogels [31-32].

3.2 Synthesis of silver nanoparticles

The biosynthesis of Ag ions into Ag atoms utilizing *Koelreuteria apiculata* extract was examined through variations in color during the synthesis process and UV-vis spectroscopy. The colloidal suspension of AgNPs suggests a color change from pale yellow to brown because of surface plasmon resonance (SPR) as shown in the inset of Fig. 2a [33-34]. The AgNPs shows an absorption band at 418 nm after 1 hour (Fig. 2a). To examine the stability of the as-prepared AgNPs with various volumes of flower extracts ranging from 1ml to 4ml were taken for studying the addition of 2 mM concentration of AgNO₃. (Fig. 2b) shows the absorption bands obtained after 2 months and indicates that SPR bands shifted slightly towards the longer wavelength region with increasing the number of days. The shift observed in the absorption peak can be influenced by the size and shape of the particle. A redshift was observed in the absorption peak with an

increase in the particle size [35]. Only a slight increase in redshift was observed after two months that confirms the stability of AgNPs.

Transmission electron microscopy (TEM) has provided insights into the formation of AgNPs. The TEM micrographs were recorded from the solution of AgNPs as shown in Fig. 3a. The figure represents the individual silver nanoparticles as well as aggregates of particles at a scale of 100 nm. Prepared AgNPs possess variable morphology and most of them were spherical in nature along with some irregular shapes. The majority of the NPs were found in the range of 20-80 nm with an average size of around 52.0 nm (Fig. 3b). A low number of particles with higher size were also noticed in some cases. There is a thin coating of the organic layer around the aggregates of small particles at a 20 nm scale, which reflects as a capping agent. At the microscopic scale, this also explains the noble dispersion of silver nanoparticles within the bio-reduced aqueous solution [36].

3.3 Characterization of synthesized hydrogels

3.3.1 FTIR spectroscopy

The FTIR spectroscopy was used to investigate the structural variations in Gum acacia, Ga-cl-poly(AAm), Ga-cl-poly(AAm-IPN-AA) and their nanocomposites as shown in Fig. 4. The gum acacia showed a broad peak at 3285 cm^{-1} that corresponds to the hydrogen-bonded OH group [37]. The peak at 2809 cm^{-1} relates to sugar, arabinose, as well as alkane and aldehyde stretching and peaks in the range of $1000\text{-}1080\text{ cm}^{-1}$ contributes to the diaryl group [38-39]. A new peak at 1650 cm^{-1} signifies -CO stretching of amide-I after graft copolymerization of AAm. The minor peak emerged at 1319 cm^{-1} assigned to -NH in-plane bending of amide-II [40-41]. The presence of new peaks signifies the grafting of polyacrylamide onto gum acacia. Further, the integration of silver nanoparticles into semi-IPN was endorsed by the characteristic peaks with lower transmittance at 3330 cm^{-1} due to the N-H stretching of protein evolving from the peptide

linkages existing in the extract and 2323 cm^{-1} due to the C=O stretching vibrations or N–H stretching vibrations. Apart from this, extra peaks with lower transmittance 2947 cm^{-1} and 2919 cm^{-1} contribute to C–H stretching of protein methylene groups were also detected [39-40]. In the case of Ga-cl-poly(AAm-IPN-AA), extra small peaks were detected at 1698 cm^{-1} and 1164 cm^{-1} due to the stretching of –CO group of acrylic acid and –COO group of the acrylate unit, respectively [42-43]. FTIR spectrum of Ga-cl-poly(AAm-IPN-AA)-AgNPs exhibits the shift of peaks towards the higher wavenumber due to the formation of covalent bonding between silver nanoparticles and electron-rich groups of the hydrogel. The occurrence of particular silver nanoparticle peaks in addition to shifting confirms the impregnation of AgNPs onto the hydrogels.

3.3.2 SEM analysis

Scanning electron micrographs were taken at different magnification to distinguish the structural variations on the surface of Gum acacia, Semi IPN and IPN. The morphology of Ga has a smooth homogenous surface (Fig 5a). Figure 5b represents the formation of the well-defined porous structure after graft copolymerization and this can be attributed to available space for water during the swollen state. The addition of poly(AA) increases the surface roughness by reducing the pore size of hydrogels (Fig 5c). The surface of IPN was highly rough in comparison to semi-IPN due to the integration of covalent bonds among different polymeric chains on crosslinking. EDX analysis was used to determine the successful synthesis of nanocomposite hydrogels along with their elemental composition. Apart from Ag, the presence of oxygen could be attributed to biomolecules that are bound on the surface of AgNPs and this corresponds to the reduction of the ionic form of silver into its elemental form [44]. In comparison, 8.73% Ag was found in Ga-cl-poly(AAm-IPN-AA)-AgNPs and 0.07% Ag was found in the case of Ga-cl-poly(AAm)-AgNPs. A comparatively less pore size of Ga-cl-poly(AAm-IPN-AA)-AgNPs in comparison to

Ga-cl-poly(AAm)-AgNPs displays the ability of IPN to impregnate a large number of silver nanoparticles (Fig. 6a and 6b).

3.3.3 XRD analysis

X-ray diffraction pattern of Gum acacia, Ga-cl-poly(AAm) and Ga-cl-poly(AAm-IPN-AA), Ga-cl-poly(AAm)-AgNPs and Ga-cl-poly(AAm-IPN-AA)-AgNPs is shown in Fig. 7. A wide maxima was obtained in gum acacia at an angle of 19° at 2θ scale with a relatively lower intensity as compared to the hydrogel samples. The shape of radiance signifies that the nature of gum acacia is moderately crystalline with dominant amorphous nature. Grafting of poly(AAm) onto gum acacia increases the relative intensity, which attributed to the enhancement of crystallinity due to the interaction of poly(AAm) with $-\text{OH}$ and $-\text{CH}$ groups of the backbone [45]. The peak maxima shifted to 20° in the 2θ scale along with a decline in diffraction peak intensity after the addition of poly(AA) onto the Ga-cl-poly(AAm), which shows the semi-crystalline nature of Ga-cl-poly(AAm). Whereas, Ga-cl-poly(AAm)-AgNPs nanocomposite exhibit an additional peak with relatively lower intensity at 38° after the impregnation of silver nanoparticles. The change in intensity indicates the interference of Ag ions in Ga-cl-poly(AAm) and this suggests the convergence of the semi-IPN network towards the disordered state. The diffractogram of Ga-cl-poly(AAm-IPN-AA)-AgNPs shows diffraction peaks at 38° , 62° , 75° , 78° in 2θ scale corresponding to diffraction scattering from the (111), (220), (220), and (311) planes, respectively. These peaks firmly indicate the fcc structure of crystalline AgNPs imbibed onto hydrogels [46]. The gradual decrease in peak intensity of Ga-cl-poly(AAm-IPN-AA) with an increase of AgNPs corresponds to a more disordered state. The relative intensity decrease was observed to be more in Ga-cl-poly(AAm-IPN-AA)-AgNPs in comparison to Ga-cl-poly(AAm)-AgNPs, which reveal that influence of AgNPs is more on nanocomposite of IPN (Fig. 7).

3.4 Antibacterial and antifungal studies

3.4.1 Antibacterial studies

Antibacterial efficiency of samples gum acacia (A), Ga-cl-poly(AAm) (B), Ga-cl-poly(AAm)-AgNPs (B1), Ga-cl-poly(AAm-IPN-AA) (C), and Ga-cl-poly(AAm-IPN-AA)-AgNPs (C1) were tested against the gram-positive (*S. aureus*) as well as gram-negative (*E. coli* and *P. aeruginosa*) bacteria (Fig. 8). Antibacterial behavior of nanocomposites was assessed against *Pseudomonas aeruginosa* at a concentration of 50 mg/ml. It was observed that nanocomposites (B1 and C1) showed enhanced antibacterial activity depicted by a clear zone of inhibition around the wells containing nanocomposite hydrogels (Fig. 8P). Antibacterial activity of nanocomposites was assessed against *E. coli* at a concentration of 50 mg/ml and it has been observed that *E. coli* was comparatively less sensitive to B1 and C1 nanocomposites in comparison to the *P. aeruginosa* (Fig. 8Q). Similarly, the antibacterial activity of nanocomposites samples (B1 and C1) was checked against *S. aureus* at concentration 50 mg/ml and sample 'A' was taken as control. The samples B, B1 and C1 exhibit moderate antibacterial activity in comparison to the *P. aeruginosa* and *E. coli* (Fig. 8S). The zone of inhibition in *S. aureus* was found to be less due to less penetrability of silver nanoparticles in the thick cell wall of Gram-positive. Whereas, the maximum zone of inhibition was witnessed in the case of *P. aeruginosa* due to different compositions of the cell wall in gram-negative bacteria. A gram-negative bacteria have a thinner cell wall made up of a looser peptidoglycan layer that allows the easy penetration of silver nanoparticles [47-49].

3.4.2 Antifungal studies

The anti-fungal activity of samples gum acacia (A), Ga-cl-poly(AAm) (B), Ga-cl-poly(AAm)-AgNPs (B1), Ga-cl-poly(AAm-IPN-AA) (C), and Ga-cl-poly(AAm-IPN-AA)-AgNPs (C1) were tested against the fungi (*Penicillium* and *Aspergillus*). The maximum zone of inhibition

was observed with sample B1 against *Penicillium* (Y) followed by sample C1 against *Aspergillus* (X) (Fig. 9). In the case of nanocomposite hydrogels, AgNPs tend to generate free radicals that cause membrane damage of the fungi. DNA condensation and dehydration are other reasons for better antifungal activity of nanocomposite hydrogels [50-51]. Less antifungal activity was observed in the case of *Aspergillus* due to the production of secondary metabolites. These metabolites interfere with the inhibitory mechanism of silver nanoparticles thereby providing resistance to AgNPs [50, 52].

4. Conclusions

Microwave-assisted synthesis of nanocomposite hydrogels was successfully carried out by the impregnation of silver nanoparticles into crosslinked hydrogels. Scanning electron micrographs displayed the change in surface morphology due to grafting of polymers onto gum acacia. The existence of silver nanoparticles in synthesized nanocomposite hydrogels was confirmed by spectroscopic techniques. Antibacterial and antifungal activities of synthesized hydrogels were studied against three bacterial and two fungal strains. The synthesized hydrogels showed varying degrees of antimicrobial activity with both bacteria and fungi. IPN nanocomposite hydrogels showed enormous potential in inhibiting the growth of bacteria as compared to semi-IPN. The varying antimicrobial activity by hydrogels might be due to the difference in the composition of the cell wall of different bacteria (peptidoglycan) and fungi (chitin, glucans and mucopolysaccharides). Also, there is a difference between the cell wall composition of Gram-negative (*P. aeruginosa* and *E. coli*) and Gram-positive (*S. aureus*). The synthesized nanocomposite hydrogels may serve as promising antimicrobial and antibiofilm agents for medical applications after their *in vitro* and *in vivo* evaluation in animal models.

Acknowledgments

One of the authors Kashma Sharma is grateful to the University Grants Commission (UGC), New Delhi, India for providing Postdoctoral Fellowship for Women [F.15-1/2017/PDFWM-2017-18-HIM-51703(SA-II)] to carry out the research. V. Sharma thanks DST, New Delhi (India) for the financial support, research project no. EMR/2016/001103.

References

- [1] M. Hamidi, A. Azadi, P. Rafiei, Hydrogel nanoparticles in drug delivery, *Adv. Drug Deliv. Rev.* 60 (2008) 1638–1649.
- [2] S.K.H. Gulrez, S.A. Assaf, G.O Phillips, *Hydrogels: Methods of Preparation, Characterization and Applications*, Progress in Molecular and Environmental Bioengineering (2011) 117-150.
- [3] X. Chen, B.D. Martin, T.K. Neubauer, R.J. Linhardt, J.S. Dordick, D.G. Rethwisch, Enzymatic and chemoenzymatic approaches to synthesis of sugar-based polymer and hydrogels, *Carbohydr. Polym.* 28 (2005) 15-21.
- [4] N. Kashyap, N. Kumar, M. Kumar, *Hydrogels for Pharmaceutical and Biomedical Applications*, *Crit. Rev. Ther. Drug.* 22 (2005)107–150.
- [5] P.H. Corkhill, C.J. Hamilton, B.J. Tighe, Synthetic hydrogels VI. Hydrogel composites as wound dressings and implant materials, *Biomater.* 10 (1989) 3-10.
- [6] M. Okada, Chemical synthesis of biodegradable polymers, *Prog. Polym. Sci.* 27 (2002) 87–133.
- [7] V. Kanikireddy, K. Kanny, Y. Padma, R. Velchuri, R. Gundeboina, B. Jagan Mohan Reddy, V. Muga, Development of alginate-gum acacia-Ag0 nanocomposites via green process for inactivation of foodborne bacteria and impact on shelf life of black grapes (*Vitis vinifera*), *J. Appl. Polym. Sci.* 136 (2018) 47331.

- [8] V.P. Padmanabhan, R. Kulandaivelu, S.N.T.S. Nellaiappan, New core-shell hydroxyapatite/Gum-Acacia nanocomposites for drug delivery and tissue engineering applications, *Mater. Sci. Eng. C* 92 (2018) 685–693.
- [9] S. Gopi, A. Amalraj, N. Kalarikkal, J. Zhang, S. Thomas, Q. Guo, Preparation and characterization of nanocomposite films based on gum arabic, maltodextrin and polyethylene glycol reinforced with turmeric nanofiber isolated from turmeric spent, *Mater. Sci. Eng. C* 97 (2019) 723–729.
- [10] K.A. Juby, C. Dwivedi, M. Kumar, S. Kota, H.S. Misra, P.N. Bajaj, Silver nanoparticle-loaded PVA/gum acacia hydrogel: Synthesis, characterization and antibacterial study, *Carbohydr. Polym.* 89 (2012) 906–913.
- [11] S.K. Bajpai, M. Kumari, A green approach to prepare silver nanoparticles loaded gum acacia/poly(acrylate) hydrogels, *Int. J. Biol. Macromol.* 80 (2015) 177–188.
- [12] S.K. Bajpai, M. Jadaun, S. Tiwari, Synthesis, characterization and antimicrobial applications of zinc oxide nanoparticles loaded gum acacia/poly(SA) hydrogels, *Carbohydr. Polym.* 153 (2016) 60–65.
- [13] A. Chaturvedi, A.K. Bajpai, J. Bajpai, K. Singh, Evaluation of poly (vinylalcohol) based cryogel-zinc oxide nanocomposites for possible applications as wound dressing materials, *Mater Sci Eng C Mater Biol Appl.* 65 (2016) 408–418.
- [14] T. Jayaramudu, K. Varaprasad, K.K. Reddy, R.D. Pyarasani, A. Akbari-Fakhrabadi, J. Amalraj, Chitosan-pluronic based Cu nanocomposite hydrogels for prototype antimicrobial applications, *Int. J. Biol. Macromol.* 143 (2020) 825–832.
- [15] A. Gilarska, J.L. Łańcucka, K. Guzdek-Zajac, A. Karewicz, W. Horak, R. Lach, K. Wójcik, M. Nowakowska, Bioactive yet antimicrobial structurally stable collagen/chitosan/lysine functionalized hyaluronic acid-based injectable hydrogels for

potential bone tissue engineering applications, *Int. J. Biol. Macromol.* 2019, In Press.
<https://doi.org/10.1016/j.ijbiomac.2019.11.052>.

[16] A.A. Al-Majed, A.R.A. Abd-Allah, A.C. Al-Rikabi, O.A. Al-Shabanah, A.M. Mostafa, Effect of oral administration of arabic gum on cisplatin-induced nephrotoxicity in rats, *J. Biochem. Mol. Toxicol.* 17 (2003) 146–153.

[17] A.R.A. Abd-Allah, A.A. Al-Majed, A.M. Mostafa, O.A. Al-Shabanah, A.G.E. Din, M.N. Nagi, Protective effect of arabic gum against cardiotoxicity induced by doxorubicin in mice: A possible mechanism of protection, *J. Biochem. Mol. Toxicol.* 16 (2002) 254–259.

[18] G.M. Fent, S.W. Casteel, D.Y. Kim, R. Kannan, K. Katti, N. Chanda, K. Katti, Biodistribution of maltose and gum arabic hybrid gold nanoparticles after intravenous injection in juvenile swine, *Nanomedicine: Nanotechnology, Biology and Medicine* 5 (2009) 128–135.

[19] K. Haraguchi, Nanocomposite hydrogel, *Curr. Opin. Solid State Mater. Sci.* 11 (2007) 47–54.

[20] S. Ahmed, S. Ullah, M. Ahmad, B.A. Swami, S. Ikram, Green synthesis of silver nanoparticles using *Azadirachta indica* aqueous leaf extract, *J. Radiat. Res. Appl. Sci.* 9 (2015) 1–7.

[21] K. Sharma, B.S. Kaith, V. Kumar, V. Kumar, S. Som, S. Kalia, H.C. Swart, Synthesis and properties of poly(acrylamide-aniline)-grafted gum ghatti based nanospikes, *RSC Adv.* 3 (2013) 25830–25839.

[22] Y. Bao, J. Ma and N. Li, Synthesis and swelling behaviors of sodium carboxymethyl cellulose-g-poly(AA-co-AM-co-AMPS)/MMT superabsorbent hydrogel, *Carbohydr. Polym.* 84 (2011) 76–82.

[23] A. Pourzavadi, H. Ghasemzadeh, H. Hosseinzadeh, Carrageenan-g-poly(acrylamide)/poly(vinylsulfonic acid, sodium salt) as a novel semi-IPN hydrogel: Synthesis, characterization, and swelling behaviour, *Polym. Eng. Sci.* 47 (2007) 1388–1395.

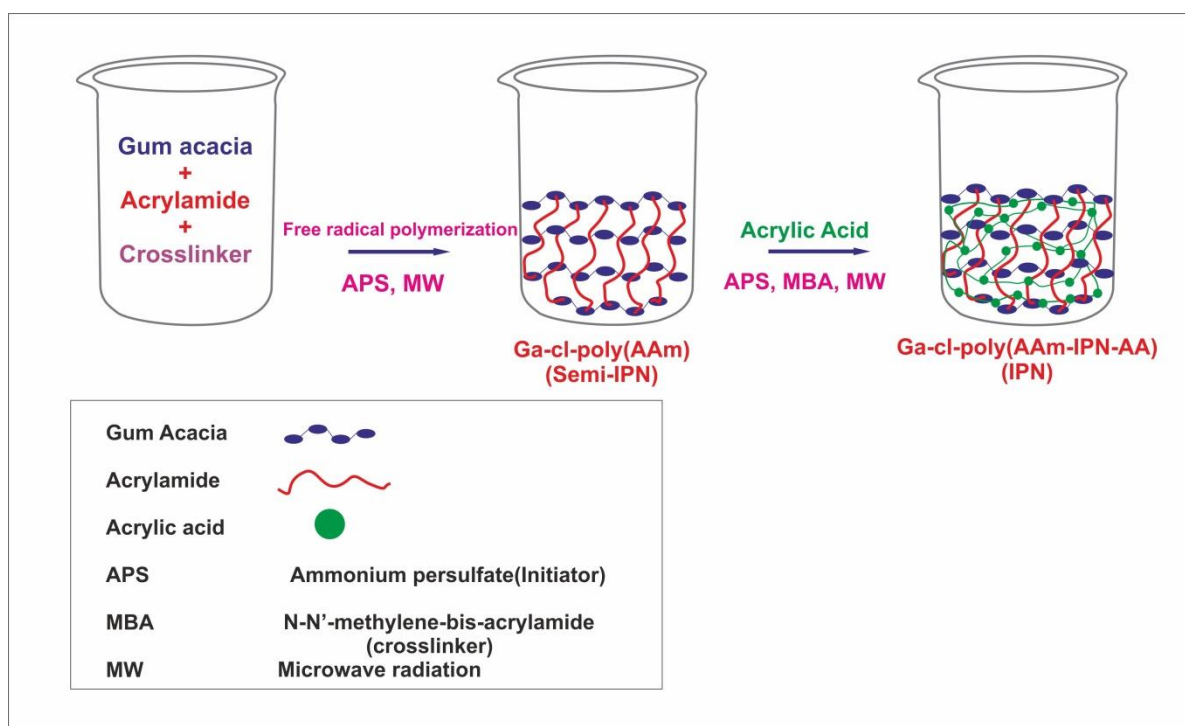
- [24] H. Mittal, S.B. Mishra, A.K. Mishra, B.S. Kaith, R. Jindal, S. Kalia, Preparation of poly(acrylamide-co-acrylic acid)-grafted gum and its flocculation and biodegradation studies, *Carbohydr. Polym.* 98 (2013) 397-404.
- [25] B.S. Kaith, R. Jindal, H. Mittal and K. Kumar, Synthesis, characterization, and swelling behavior evaluation of hydrogels based on Gum ghatti and acrylamide for selective absorption of saline from different petroleum fraction–saline emulsions, *J. Appl. Polym. Sci.* 124 (2012) 2037-2047.
- [26] S. Pal, S. Ghorai, M. Dash, S. Ghosh and G. Udayabhanu, Flocculation properties of polyacrylamide grafted carboxymethyl guar gum (CMG-g-PAM) synthesised by conventional and microwave assisted method, *J. Hazard. Mater.* 192 (2011) 1580 -1588.
- [27] S.S. Samandari, M. Gazi, E. Yilmaz, UV-induced synthesis of chitosan-g-polyacrylamide semi-IPN superabsorbent hydrogels, *Polym. Bull.* 68 (2012) 1623-1639.
- [28] O. Garcia, M.D. Blanco, C. Gomez, J.M. Teijon, Effect of the crosslinking with 1,1,1-trimethylolpropane trimethacrylate on 5-fluorouracil release from poly(2-hydroxyethyl methacrylate) hydrogels, *Polym. Bull.* 38 (1997) 55-62.
- [29] C. Silioc, A. Maleki, K. Zhu, A.L. Kjniksen, B. Nyström, Effect of Hydrophobic Modification on Rheological and Swelling Features during Chemical Gelation of Aqueous Polysaccharides, *Biomacromolecules* 8 (2007) 719-728.
- [30] K. Kabiri, M.J. Zohuriaan-Mehr, Superabsorbent hydrogel from concentrated solution Terpolymerization, *Iran Polym. J.* 13 (2004) 423-430.
- [31] A.K. Bajpai, M. Shrivastava, Dynamic swelling behavior of polyacrylamide based three component hydrogel, *J. Macromol. Sci.* 37 (2000) 1069-1088.
- [32] B. Singh, M. Vashishtha, Development of novel hydrogels by modification of sterculia gum through radiation cross-linking polymerization for use in drug delivery, *Nucl. Instr. Meth. Phys. Res. B.* 266 (2008) 2009–2020.

- [33] T. Edison, M. Sethuraman, Instant green synthesis of silver nanoparticles using *Terminalia chebula* fruit extract and evaluation of their catalytic activity on reduction of methylene blue, *Process Biochem.* 47 (2012) 1351-1357.
- [34] P. Velusamy, J. Das, R. Pachaiappan, B. Vaseeharan, K. Pandian, Greener approach for synthesis of antibacterial silver nanoparticles using aqueous solution of neem gum (*Azadirachta indica* L.), *Ind. Crops Prod.* 66 (2015) 103–109.
- [35] Y. Xia and N.J. Halas, Shape-controlled synthesis and surface plasmonic properties of metallic nanostructures, *MRS Bull.* 30 (2005) 338–348.
- [36] P. Kouvaris, A. Delimitis, V. Zaspalis, D. Papadopoulos, S.A. Tsipas, N. Michailidis, Green synthesis and characterization of silver nanoparticles produced using *Arbutus Unedo* leaf extract. *Mater. Lett.* 76 (2012) 18–20.
- [37] I.M. Khan, S. Shakya, N. Singh, Preparation, single-crystal investigation and spectrophotometric studies of proton transfer complex of 2, 6-diaminopyridine with oxalic acid in various polar solvents, *J. Mol. Liq.* 250 (2018) 150-161.
- [38] R.M.A. Daoub, A.H. Elmubarak, M. Misran, E.A. Hassan, M.E. Osman, Characterization and functional properties of some natural Acacia gums, *J. Saudi Soc. Agric. Sci.* 17 (2018) 241-249.
- [39] B.A. Aderibigbea, K. Varaprasadb, E.R. Sadikub, S.S. Rayd, X.Y. Mbiandae, M.C. Fotsinge, S.J. Owonubib, S.C. Agwunchab, Kinetic Release Studies of nitrogen-containing bisphosphonate from gum Acacia Crosslinked hydrogels, *Int. J. Biol. Macromol.* 73 (2015) 115–123.
- [40] S. Marimuthu, A.A. Rahuman, G. Rajakumar, T. Santhoshkumar, A.V. Kirthi, C. Jayaseelan, C. Kamaraj, Evaluation of green synthesized silver nanoparticles against parasites, *Parasitol. Res.* 108 (2010) 1541–1549.

- [41] N. Singh, I.M. Khan, A. Ahmad, S. Javed, Synthesis, spectrophotometric and thermodynamic studies of charge transfer complex of 5,6-dimethylbenzimidazole with chloranilic acid at various temperatures in acetonitrile and methanol solvents, *J. Mol. Liq.* 221 (2016) 1111-1120.
- [42] S.M. Ghaseminezhad, S. Hamed, S.A. Shojaosadati, Green synthesis of silver nanoparticles by a novel method: Comparative study of their properties, *Carbohydr. Polym.* 89 (2012) 467-472.
- [43] P. Banerjee, M. Satapathy, A. Mukhopadhyay, P. Das, Leaf extract mediated green synthesis of silver nanoparticles from widely available Indian plants: synthesis, characterization antimicrobial property and toxicity analysis, *Bioresour Bioprocess* 3 (2016).
- [44] S. Kaviya, J. Santhanalakshmi, B. Viswanathan, J. Muthumary, K. Srinivasan, Biosynthesis of silver nanoparticles using citrus sinensis peel extract and its antibacterial activity, *Spectrochim. Acta. A Mol. Biomol. Spectrosc.* 79 (2011) 594-598.
- [45] B.S. Kaith, R. Sharma, K. Sharma, S. Choudhary, V. Kumar, S.P. Lochab, Effects of O_7^+ and Ni^{9+} swift heavy ions irradiation on polyacrylamide grafted Gum acacia thin film and sorption of methylene blue, *Vac.* 111 (2015) 73-82.
- [46] R. Kalaivani, M. Maruthupandy, T. Muneeswaran, A. Hameedha Beevi, M. Anand, C.M. Ramakritinan, A.K. Kumaraguru, Synthesis of chitosan mediated silver nanoparticles (Ag NPs) for potential antimicrobial applications, *Frontiers in Laboratory Medicine* 2 (2018) 30-35.
- [47] L. Gao, L. Wang, L. Yang, Y. Zhao, N. Shi, C. An, Y. Sun, J. Xie, H. Wang, Y. Song, Y. Ren, Preparation, characterization and antibacterial activity of silver nanoparticle/graphene oxide/diatomite composite, *Appl. Surf. Sci.* 484 (2019) 628-636.

- [48] I.M. Khan, A. Ahmad, M. Oves, Synthesis, characterization, spectrophotometric, structural and antimicrobial studies of the newly charge transfer complex of p-phenylenediamine with π acceptor picric acid, *Spectrochim. Acta A Mol. Biomol. Spectrosc.* (2010) 1059-1064.
- [49] A. Bal, F.E. Çepni, O. Çakir, I. Acar and G. Güçlü, Synthesis and Characterization Of Copolymeric And Terpolymeric Hydrogel-Silver Nanocomposites Based On Acrylic Acid, Acrylamide And Itaconic Acid: Investigation of Their Antibacterial Activity Against Gram-Negative Bacteria, *Braz. J. Chem. Eng.* 32 (2015) 509 - 518.
- [50] Zulkarnain, I.M. Khan, A. Ahmad, L. Miyan, M. Ahmad, N. Azizc, Synthesis of charge transfer complex of chloranilic acid as acceptor with p-nitroaniline as donor: Crystallographic, UV–visible spectrophotometric and antimicrobial studies, *J. Mol. Struct.* 1141 (2017) 687-697.
- [51] K.M. Alananbeh, W.J. Al-Refae, Z. Al-Qodah, Antifungal Effect of Silver Nanoparticles on Selected Fungi Isolated from Raw and Waste Water, *Ind. J. Pharm. Sci.* 79 (2017) 559-567.
- [52] A. Kujumgiev, I. Tsvetkova, Yu. Serkedjieva, V. Bankova, R. Christov, S. Popov, Antibacterial, antifungal and antiviral activity of propolis of different geographic origin, *J. Ethnopharmacol.* 64 (1999) 235–240.

Schemes and Figures:



Scheme 1: Synthesis of Ga-cl-poly(AAm) and Ga-cl-poly(AAm-IPN-AA).

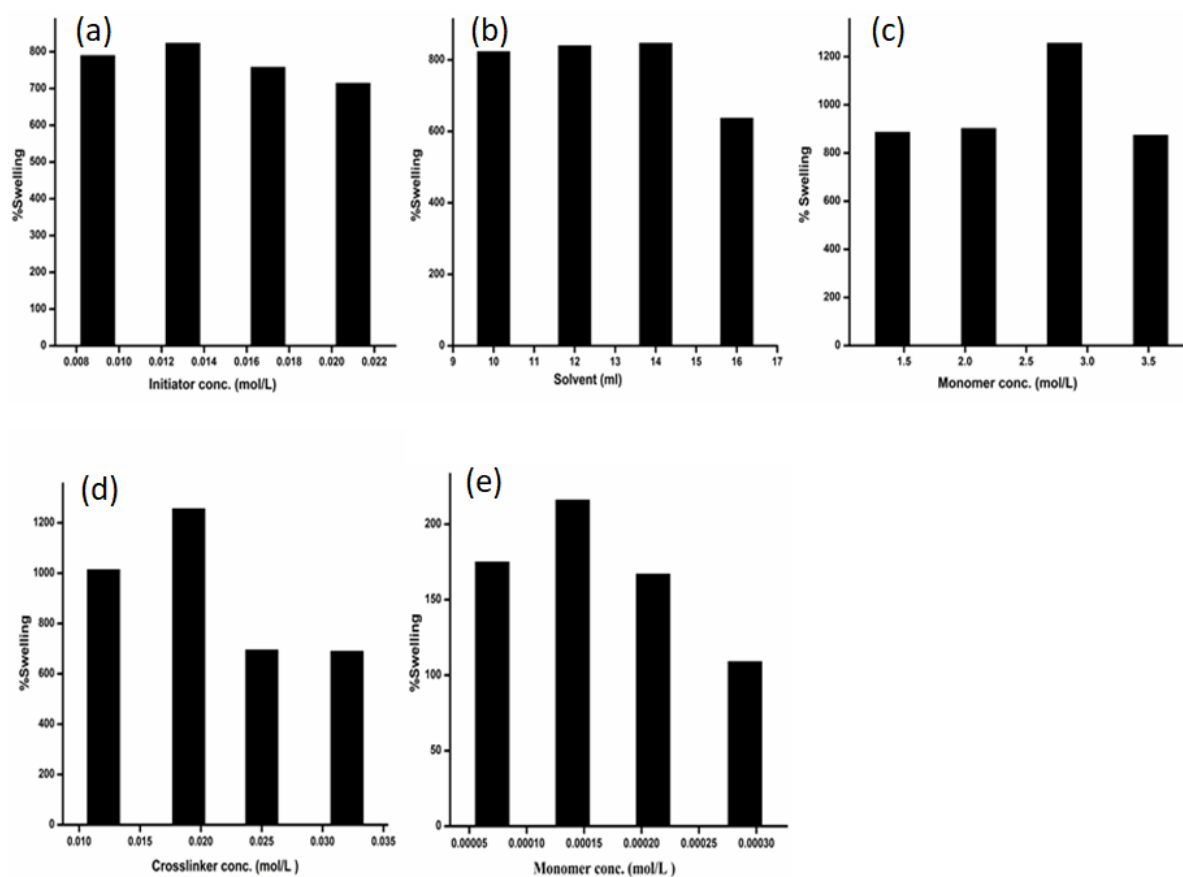


Figure 1: Variation of percent swelling with (a) initiator concentration, (b) amount of solvent, (c) monomer (AAm) concentration, (d) crosslinker concentration, and (e) monomer (AA) concentration.

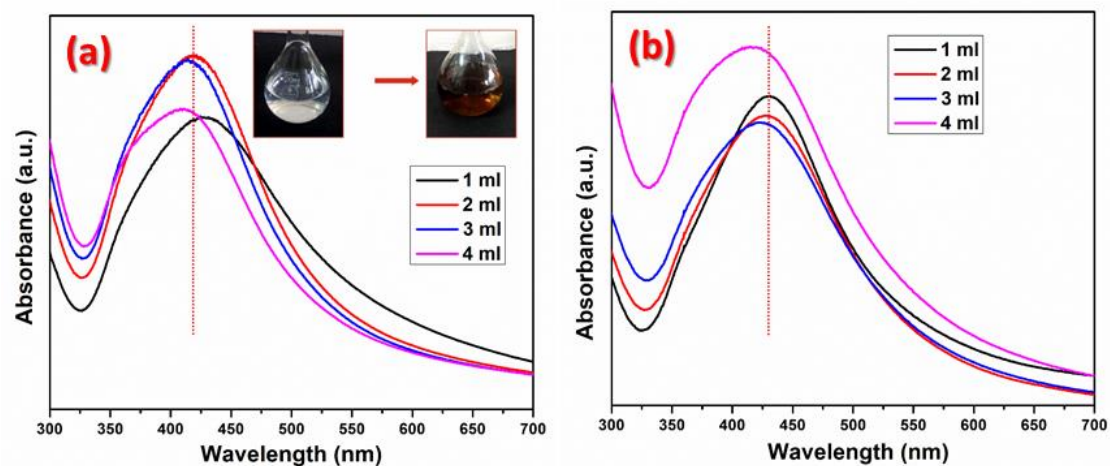


Figure 2: UV visible spectra of silver nanoparticles with different flower extract concentrations after (a) 1 hour (b) 2 months.

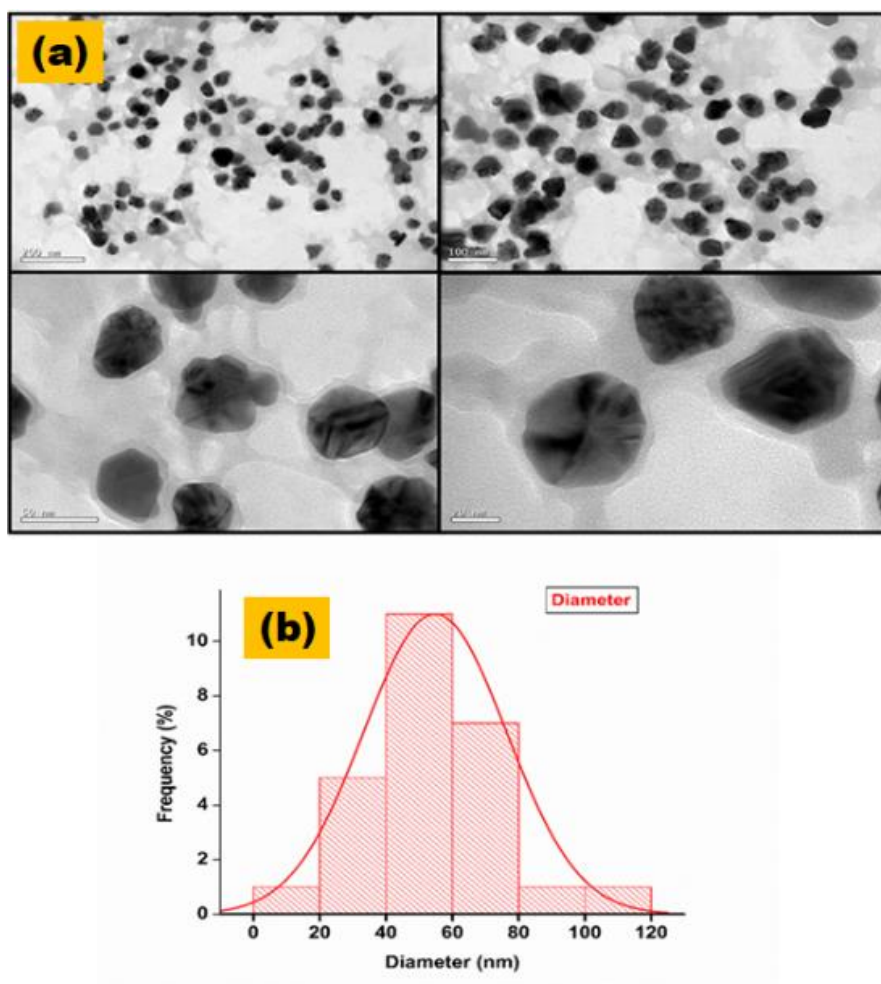


Figure 3: (a) Transmission electron microscopic analysis of AgNPs at various resolutions and (b) size distribution histogram of AgNPs.

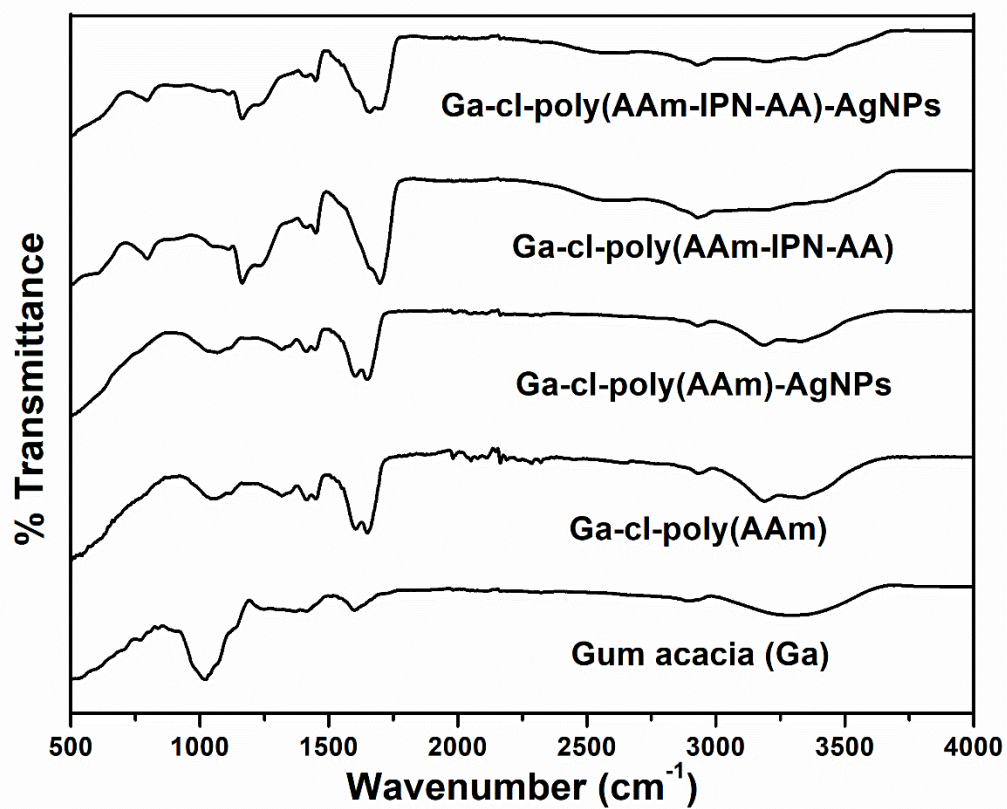


Figure 4: FTIR spectra of Gum acacia, Ga-cl-poly(AAm), Ga-cl-poly(AAm)-AgNPs, Ga-cl-poly(AAm-IPN-AA) and Ga-cl-poly(AAm-IPN-AA)-AgNPs.

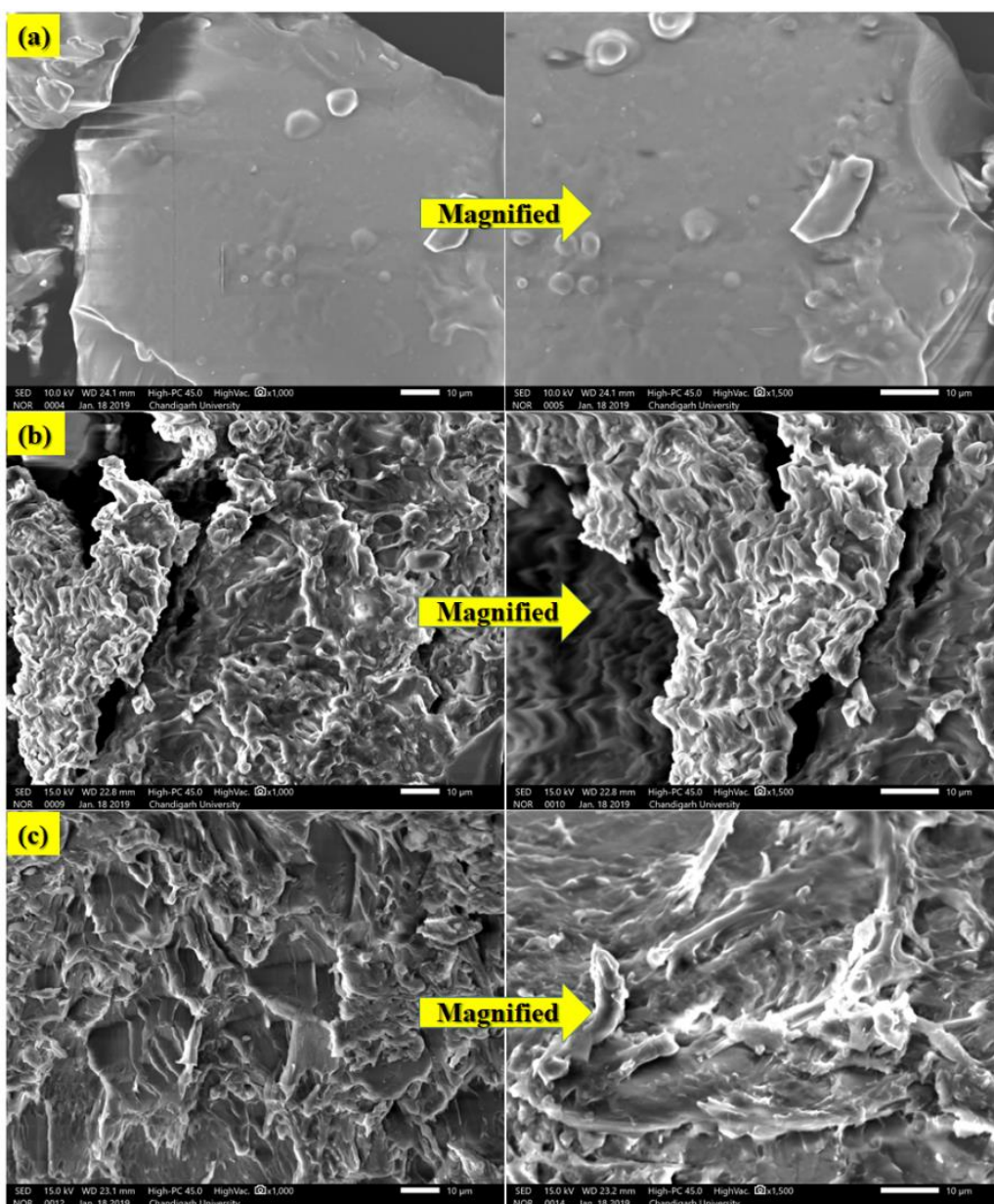


Figure 5: Surface morphology micrographs of (a) Gum acacia, (b) Ga-cl-poly(AAm), and (c) Ga-cl-poly(AAm-IPN-AA).

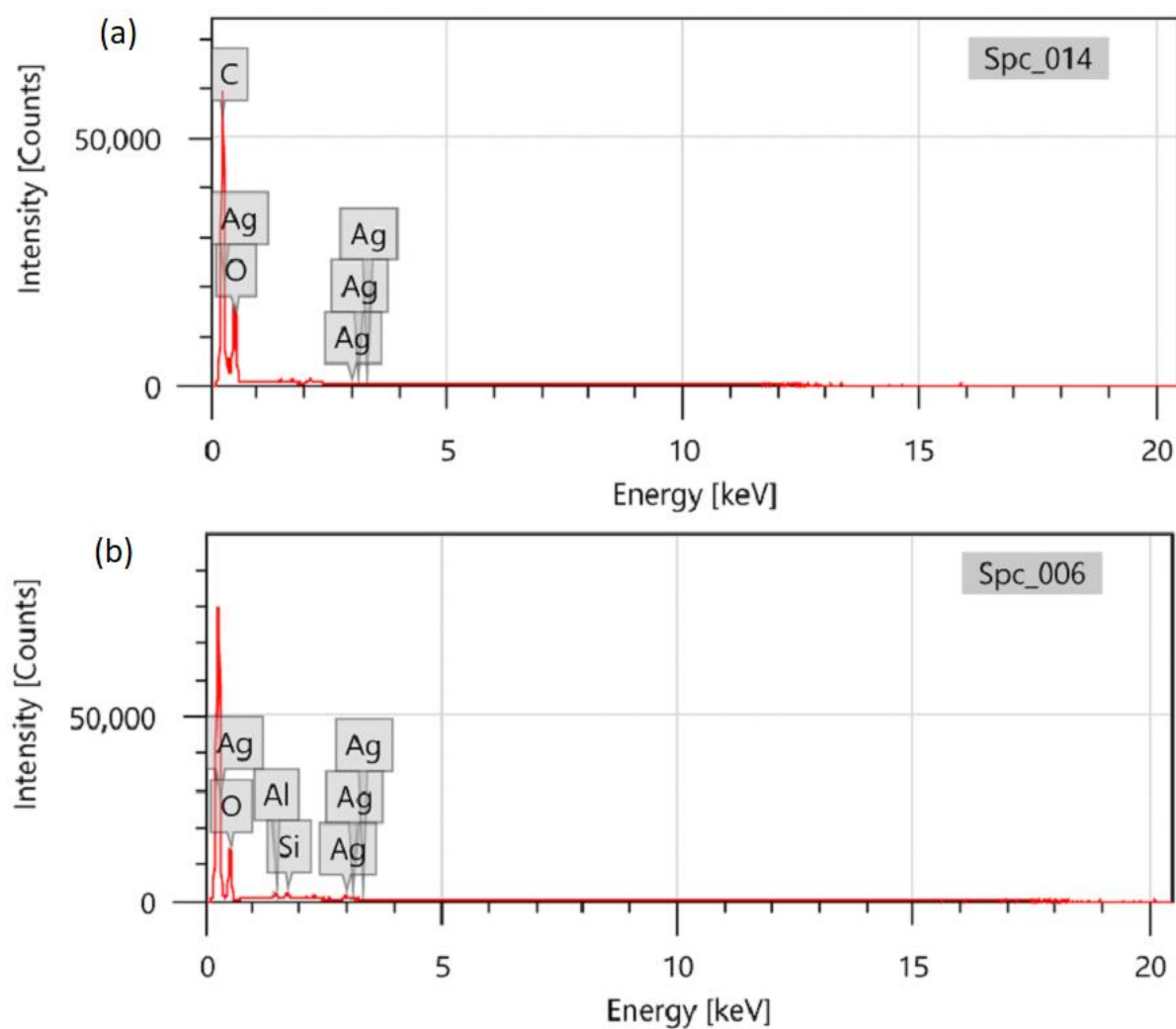


Figure 6: EDX spectra of (a) Ga-cl-poly(AAm)-AgNPs and (b) Ga-cl-poly(AAm-IPN-AA)-AgNPs.

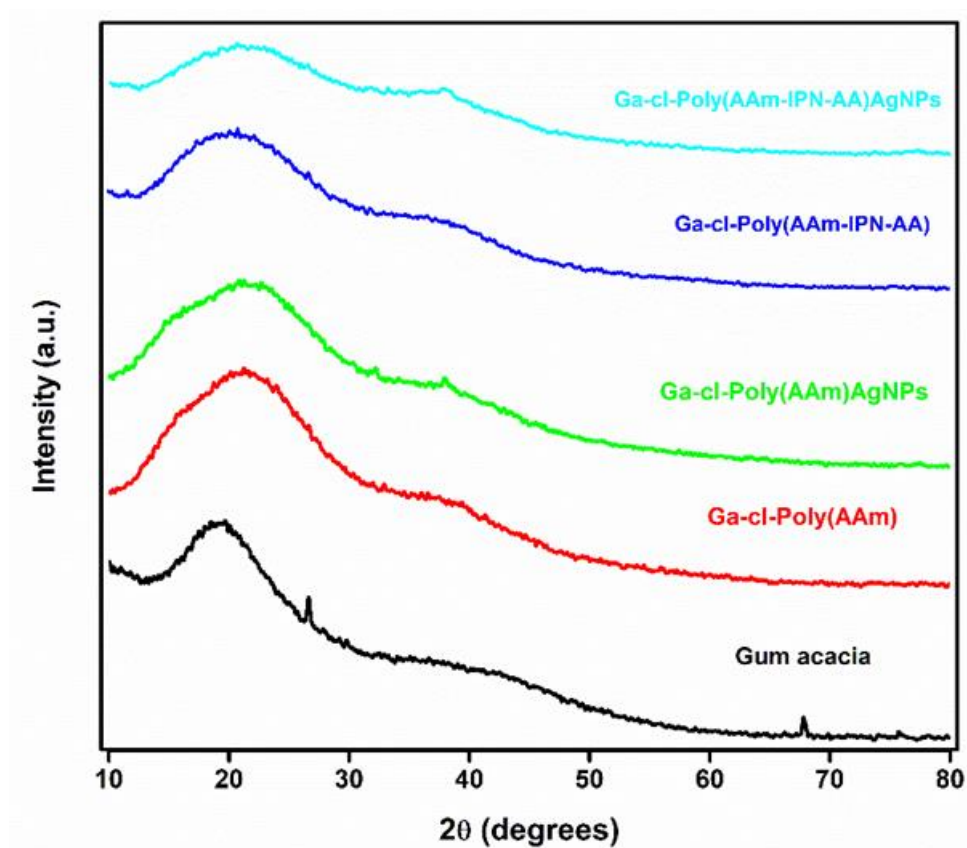


Figure 7: XRD pattern of Gum acacia, Ga-cl-poly(AAm), Ga-cl-poly(AAm)-AgNPs, Ga-cl-poly(AAm-IPN-AA), and Ga-cl-poly(AAm-IPN-AA)-AgNPs.

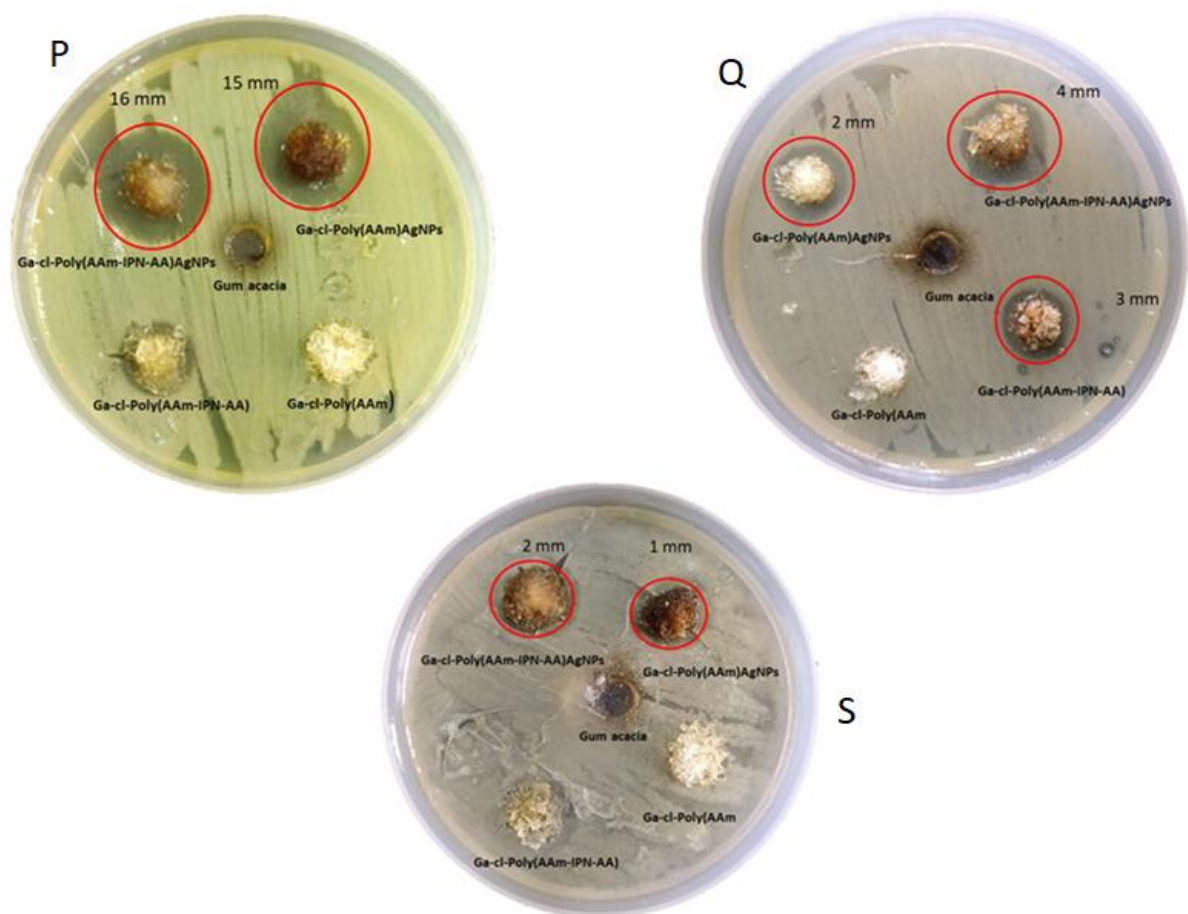


Figure 8: MHA plates having an antibacterial activity of test samples (A, B, B1, C, C1) against bacterial strains, *Pseudomonas aeruginosa* (P), *Escherichia coli* (Q) and *Staphylococcus aureus* (S).

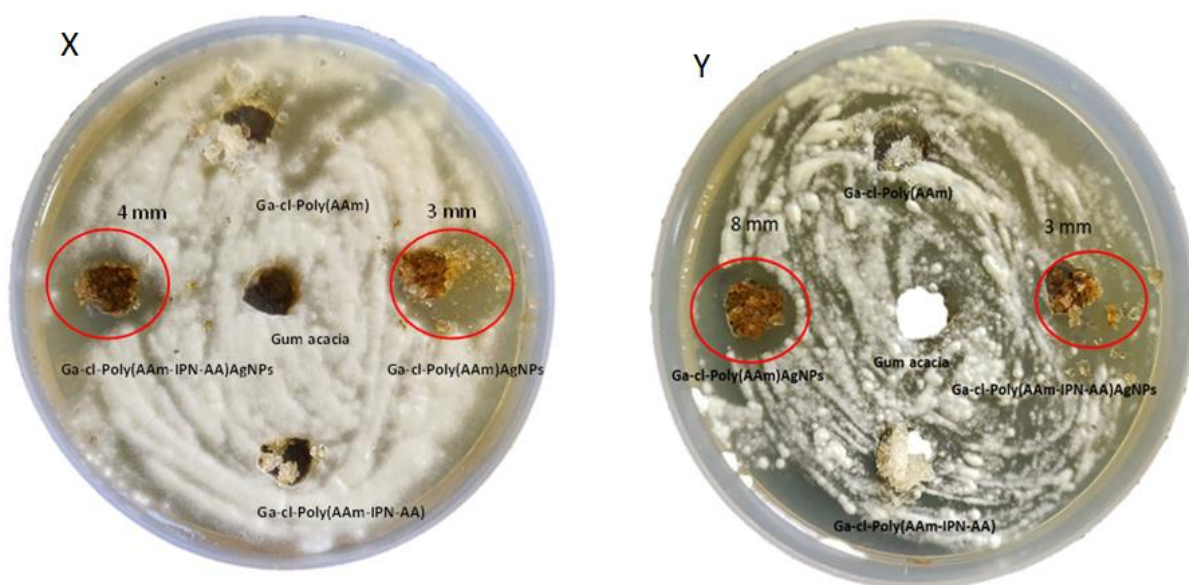


Figure 9: PDA plates having an antifungal activity of test samples (A, B, B1, C, C1) against fungal strains, *Aspergillus* (X) and *Penicillium* (Y).